Preparation of multi-hydroxy chitosan derivative and its synergistic effect on fire performance and mechanical properties of epoxy resin

Jing Yan [a, b, 1], Haiqing Jiang [a, 1], Na Gao [a], Xiangnan Zhang [a], Xingyu Liu [a], Siqi Huo [c], Jing Lu [a, *], Junjie Wang [a, *]

[a] School of Bioengineering and Health, Hubei Key Laboratory for New Textile Materials and Applications, Key Laboratory of Textile Fiber and Products, Ministry of Education, Wuhan Textile University, Wuhan 430200, PR China

[b] Emergency control center, Jingzhou Administration of Work Safety, Jingzhou 434007, PR China

[c] School of Engineering, University of Southern Queensland, Center for Future Materials, University of Southern Queensland, 4300 Springfield Central Queensland, Australia

[1] These authors contributed equally to this work.

[*]**Corresponding authors:**

Junjie Wang, School of Bioengineering and Health, Hubei Key Laboratory for New Textile Materials and Applications, Wuhan Textile University, Wuhan 430200, PR China. Email: wjjdjgky@163.com

Jing Lu, Key Laboratory of Textile Fiber and Products, Ministry of Education, Wuhan Textile University, Wuhan 430200, PR China. Email: jlu@wtu.edu.cn

Abstract

A chitosan derivative, named as HCS, was synthesized by a simple reaction of para-hydroxybenzaldehyde with chitosan (CS), and was then used in combination with 9, 10-dihydro-9-oxa-10-phenanthrene-10-oxide (DOPO) to obtain a biomass-based intumescent flame retardant (IFR) in epoxy resins (EPs). At a total addition of 5 mass% and a mass ratio of DOPO to HCS being 3:1, the modified EP (S4) successfully passed the vertical combustion (UL-94) V-0 rating with a limit oxygen index (LOI) value of up to 33.0 %. CC tests showed a 21.6 % reduction in both peak smoke production rate (PSPR) and peak heat release rate (PHRR), and 71.4 % reduction in total smoke production (TSP) for sample S4 compared with EP. Ulteriorly, XPS, FTIR, SEM and Raman tests were performed on the char residues of different modified samples after CC tests. These results showed that the char residue of sample S4 had an intact and dense structure, which played a role in preventing hot and gas exchange. In a word, the combination of HCS and DOPO imparted better flame retardancy properties to the epoxy resin than the singular use of them. Additionally, the mechanical properties of the modified EPs were not impaired by the addition of HCS and DOPO.

Keywords Flame retardant · Epoxy resin · Chitosan derivative · DOPO

Introduction

Currently, epoxy resins (EPs) have been widely applied in aerospace, coatings, construction, and other industrial fields due to its great mechanical strength and superior chemical stability [1-3]. However, PEs show intrinsic and high flammability with a LOI value of about 21.6%, which greatly limits its industrial application as high-performance materials [4]. In this regard, the development of EPs with flame retardant properties is particularly important in both academe and industry [5].

The common strategies used to improve the flame retardant of EPs are mainly focus on the reactive flame-retardant modification and additive flame-retardant modification. Reactive flame-retardant modification usually changes the curing process of EP, which affects its thermal stability after curing. However, the preparation procedure of reactive flame retardancy EPs is complicated and the reaction conditions are extremely rigorous, making it difficult to achieve large-scale industrial production [6, 7]. Thus, the modified method of additive flame retardant is the most widely adopted to enhance the flame retardant of EP due to the low cost, simple use, and high efficiency. Although the mechanical property of the material, modified by the additive flame retardant, is negatively affected. A good dispersion of the flame retardant in the EPs matrix can solve this problem, which is contributed to achieve a high degree of compatibility [8, 9]. In the regard, the additive flame-retardant modification is

considered as the most effective method for improvement of the flame retardant of EP in modern industrial production [10, 11].

Over the years, a classical phosphorus-containing compounds, such as DOPO and its derivatives, have been extensively studied and used in the flame retardancy of EPs. Huo et al. synthesized a hyperbranched phosphorus-nitrogen-boron-containing DOPO derivative, named as BDHDP. The addition of BDHDP at less than 3.0 mass% not only increased the glass transition temperature of EPs, but also maintained the optical transmittance. In addition, the mechanical strength and toughness of the modified EPs were improved, meanwhile, the dielectric constant and losses were reduced [12]. Wang et al. designed a multifunctional curing agent polyethyleneimine (PES) for EP. The addition of PES improved the high visible light transmission of the EPs and the UV shielding properties. The LOI value was 35.0 % and obtained UL-94 V-0 rating at the addition of 30 mass% PES into EPs. Excellent flame retardant, smoke suppression and mechanical properties were achieved for the modified EPs with PES [13]. Shi et al. used trichlorovinylsilane, triethylenetetramine and DOPO as raw materials to synthesize a flame retardant hyperbranched polymer TTD. At a lower TTD addition (≤ 4 mass%), the EP/TTD samples showed higher transparency, glass transition temperature and well UV-barrier properties than unmodified sample. Meanwhile, the mechanical properties of EP/TTD were also increased. The LOI value for the EP with 7

mass% TTD sample was up to 40.0 %, which had passed the UL-94 V-0 rating [14]. A bio-based phosphorus-containing benzoxazine monomer (SFD-BOZ) was synthesized by Cao et al. via a two-step reaction using salicylaldehyde, furfuryl amine, paraformaldehyde, and DOPO. When 20.7 mass% of SFD-BOZ was added to the EP/Methyltetrahydrophthalic anhydride system, the modified EPs had a LOI value of 35.2 % and achieved the UL-94 V-0 rating. Meanwhile, the mechanical properties were improved [15]. Although all these above DOPO derivatives endow EPs with good flame retardancy properties, DOPO is rather expensive and its derivatives were synthesized in minimum two steps.

In order to reduce costs, energy consumption, and the amount of phosphorus added, this work was considered to incorporate DOPO, which has good flame retardancy properties, jointly with other structurally simple and inexpensive compounds, as an IFR for EPs. Hu et al. used chicken feather keratin (CK) with DOPO to modify the EPs, which obtained good flame retardancy at a total addition of 20 mass% of DOPO and CK [16]. Yang et al. used a synergistic flame-retardant system consisting of expansible graphite (EG) and DOPO. With the addition of 14 mass% EG, 6 mass% DOPO, and a phosphorus content of 0.86 mass%, the modified EPs achieved an LOI value of 38 % and successfully passed UL-94 V-0 rating [17].

Wang et al. prepared a new flame retardant, poly (aluminum hexamethylene hypophosphonate) (APHP), and incorporated it into EP with DOPO. The

2%APHP/4%DOPO/EP (P content of 0.98 mass%) thermoset resin had a higher LOI value and a higher UL-94 rating than the thermoset resin with 6 mass% APHP and 6 mass% DOPO alone. The CC test results showed a lower PHRR and less THR. It indicated that there was a significant synergistic effect between APHP and DOPO [18]. A novel flame retardant, containing silicon and nitrogen (PSiN), was synthesized by Zhang et al., and it was used together with DOPO to prepare a flame-retardant system for EP. When 7 mass% DOPO and 3 mass% PSiN were incorporated, the LOI value of modified EP was up to 34 %, and passed the UL-94 V-0 rating [19]. Zeng et al. adopted organotitanate (Ti) and DOPO directly for epoxy resin of flame retardancy. When 4 mass% Ti and 10 mass% DOPO were added to the epoxy resin (P-content is 1.4%), the EP/Ti/DOPO system reached UL-94 V-0 rating with an LOI value of 34.7 % [20]. Luo et al. synthesized the flame-retardant tris (3-nitrophenyl) phosphine (NPPh3) for the flame retardancy of epoxy resins. The results showed that the flame retardancy of the modified thermosetting resin was enhanced and the LOI value of the sample 2%NPPh3/4%DOPO/EP was 33.8 % and the UL-94 test achieved V-0 rating. The combination of NPPh3 and DOPO resulted in a higher flame retardancy efficiency and high temperature thermal stability for EP [21].

Chitosan, which is a cationic polyelectrolyte produced by deacetylation of chitin, is abundant in nature, and it can be used as a good carbon source for IFRs. However, chitosan

has poor thermal stability itself and easily oxidizes and discolors or even carbonizes at high temperatures, thus it is necessary to enhance its thermal stability to cater for the curing conditions of EPs. Unlike our previous works [22, 23], aldehydes containing hydroxyl substituents were selected to be reacted with chitosan via a simple condensation reaction to obtain a chitosan derivative, namely HCS. HCS was then in combination with DOPO to be the IFR for EPs. The modified EPs showed a significant improvement in both flame retardancy and mechanical properties.

Experimental

Materials

DOPO and p-hydroxybenzaldehyde were obtained from Shanghai Aladdin Bio-Chem Technology Co., LTD, Shanghai, China. Ethanol, tetrahydrofuran and Diamino diphenylmethane (DDM) were purchased from Macklin Chemical Reagent Co., Ltd, Shanghai, China. Chitosan (The average molecular weight of 108735 g mol^{-1}, degree of deacetylation is 95.83 %) was obtained from Macklin Reagent Co., LTD, Shanghai, China. Epoxy resin (E-44, DGEBA) was provided by Nantong Xingchen Synthetic Materials Co., LTD, Jiangsu, China.

Synthesis of HCS

As shown in Fig. 1(a), HCS was successfully synthesized according to the literature methods

and our pre-works [23-25]. Firstly, chitosan (0.1 mol, 16.57 g) was homogeneously dispersed in 250 mL of ethanol in a reactor with a mechanical agitator and condenser. Then, p-hydroxybenzaldehyde (0.1 mol, 12.212 g) was dissolved in 50 mL of tetrahydrofuran and titrated over 30 min using a constant pressure funnel. The mixture was heated to 80 °C and refluxed for 12 h. The resulting mixture was cooled and filtered, then the resulting filter cake was washed three times with methanol. Finally, the product was dried under vacuum at 60 °C for 6 h. The pure product HCS was obtained.

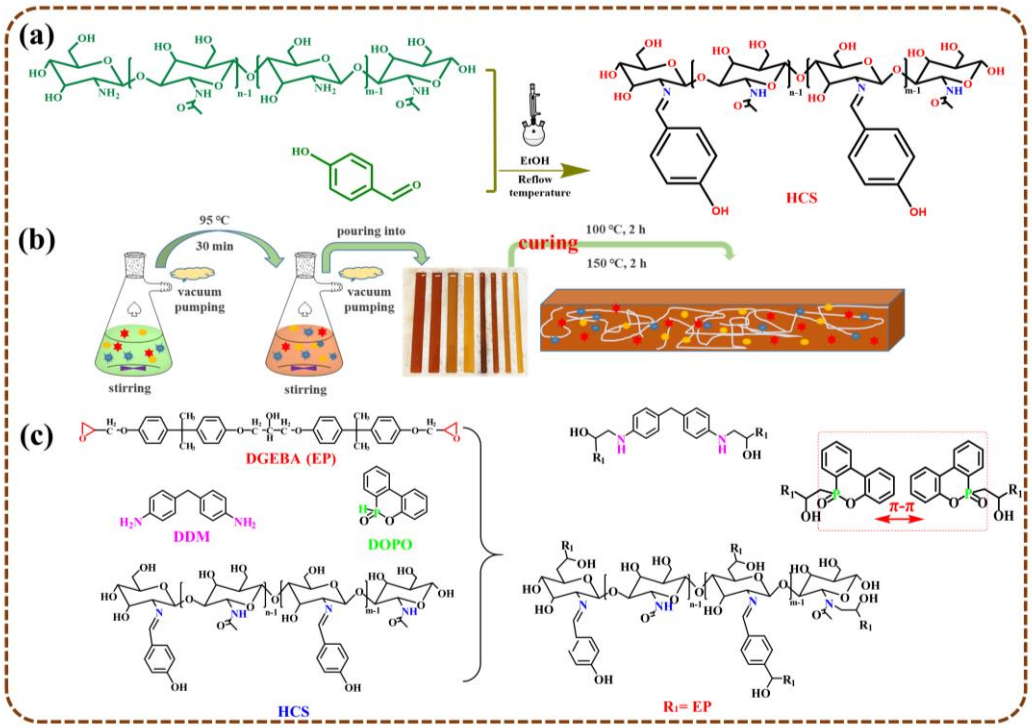

Fig. 1 (**a**) Synthetic route of HCS, (**b**) preparation process of EP composites, and (**c**) the possible interactions between HCS/DOPO and EP

Preparation of flame retardancy composite materials

Flame retardancy EP composites were prepared between DOPO, HCS, DGEBA and DDM by

thermal curing reaction. As seen in Fig. 1(b), at 95 °C, DGEBA and HCS were mixed thoroughly in a single flask containing a pumping nozzle to obtain a translucent liquid. DOPO was then added in a certain mass ratio and stirred vigorously to make it homogeneous. After about 30 minutes DDM was added and the mixture was stirred continuously under vacuum. Finally, the mixture was poured into preheated clean Teflon molds while still hot and cured (2 h at 100 °C and a further 2 h at 150 °C).

Table 1 showed the stoichiometric formulations of the DGEBA/HCS/DOPO/DDM systems at different amounts, together with the corresponding numbers. S0 represents a neat EP sample, S1 represents an EP sample with 8 mass% DOPO, S2 represents an EP sample with 8 mass% HCS, S3 represents an EP sample with a total addition of 3 mass% HCS and DOPO, where the mass ratio of HCS to DOPO is 1:3, S4 represents an EP sample with a total addition of 5 mass% HCS and DOPO, where the mass ratio of HCS to DOPO is 1:3, S5 represents an EP sample with 8 mass% total addition of HCS and DOPO where the mass ratio of HCS to DOPO is 1:3, S6 represents an EP sample with 5 mass% DOPO addition and S7 represents an EP sample with 5 mass% HCS addition.

Table 1 Stoichiometric formulas of epoxy thermosets.

Samples	Formulation (mass%)				P-content
	EP (g)	DOPO (g)	HCS (g)	DDM (g)	(%)

S0	25.05	0	0	6.52	0
S1 (8 mass%)	25.05	2.74	0	6.52	1.14
S2 (8 mass%)	25.05	0	2.74	6.52	0
S3 (3 mass%, 1:3)	25.03	0.73	0.24	6.51	0.32
S4 (5 mass%, 1:3)	25.06	1.24	0.41	6.50	0.53
S5 (8 mass%, 1:3)	25.08	2.06	0.69	6.53	0.86
S6 (5 mass%)	25.05	1.66	0	6.52	0.72
S7 (5 mass%)	25.05	0	1.66	6.52	0

Samples characterization

FT-IR Analysis. A German Thermo Nicolet 5700 infrared spectrometer was used. The samples were examined after KBr compression of HCS and char residue from the combustion of modified epoxy resin.

Elemental analysis. The samples were analyzed for C, H and N using a Vario MACRO type elemental analyzer.

Thermogravimetric analysis (TGA). TGA referred to the analysis of the thermal stability of the polymer by thermogravimetric analyzer. The thermal stability of the polymer was analyzed by Germany NETZSCH STA449F3 thermogravimetric analyzer. The heating rate

was 10 ℃, the heating range was 40-700 ℃, and the nitrogen flow rate was 50 mL min^{-1}.

LOI test. The HC-2C oxygen index meter was used to maintain the minimum percentage oxygen content of the burning sample according to ASTM D2863-97. The sample size was 130 mm × 6.5 mm × 3 mm.

Vertical flame tests. The CZF-4 vertical burner was used to test the materials according to ASTM D3801 test standard with a specimen's dimension of 130 mm × 13 mm× 3 mm.

CC tests. According to ISO 5660 standard, the combustion and charring behavior of samples were studied by using FTT0007 cone calorimeter. The test heat flux was 35 kW m^{-2}. Sample size was 100 mm × 100 mm × 3.2 mm.

Raman spectroscopy (Raman). Raman spectra were observed at room temperature by a LabRAMHR800 laser Raman spectrometer (SPEX Co.) with a 532 nm He-Ne laser line.

Scanning electron microscope (SEM). INSPECT F scanning electron microscope was used to observe and analyze the surface microstructure of the carbon residue after combustion.

Pyrolysis GC/MS analysis. Py-GC/MS analysis of the target products was obtained by a combination of a pyrolizer (CDS 5200) and a gas chromatograph-mass spectrometer (Perkin-Elmer Clarus 680 GCSQ8MS). Using helium as the carrier gas, the injection temperature was held at 40 °C for 3 min, then heated to 280 °C and held at 280 °C for 5 min. The GC/MS interface temperature was 280 °C and the cracking temperature to 600 °C. Under

electron bombardment, the electron energy was 70 eV and the ion source temperature was kept at 250 °C.

Thermogravimetric analysis/infrared spectroscopy (TG-FTIR) analysis. TG-FTIR was carried out on an STA 449F3 instrument to analyze the FTIR spectra of the gaseous components in TGA. An approximately constant mass of sample (10.0 mg) was placed in an alumina crucible and heated from 30 °C to 800 °C. The heating rate was 10 °C min^{-1} and the flow rate were 60 mL min^{-1} under a nitrogen atmosphere.

Mechanical properties testing. The tensile and non-notched impact tests were undertaken on a CMT4104 universal testing machine and a ZBC1251 pendulum impact tester, respectively (reference standards: GB/T 1040.2-2006, GB/T 9341-2008 and GB/T 1843-2008). The tensile specimen size was 75 mm × 4 mm × 2 mm and was dumbbell shaped. Three-point bending specimens were rectangular in shape 80 mm × 10 mm × 4 mm. A minimum of three specimens were tested per sample and the average value was taken.

Results and discussion

Structural characterization and elemental analysis of HCS

The infrared spectrum analysis results of HCS were shown in Fig. 2(a). The characteristic peaks of sugar structure and amino group at 894, 1160 and 1603 cm^{-1} can be observed from the infrared spectrum of CS [26, 27]. After the chemical modification, a new peak attributed

to -C=N- can be detected near 1635 cm^{-1}, which can prove the production of Schiff base [28]. The additional peaks near 1500 and 833 cm^{-1} in HCS were assigned to the phenyl group in the molecule [29].

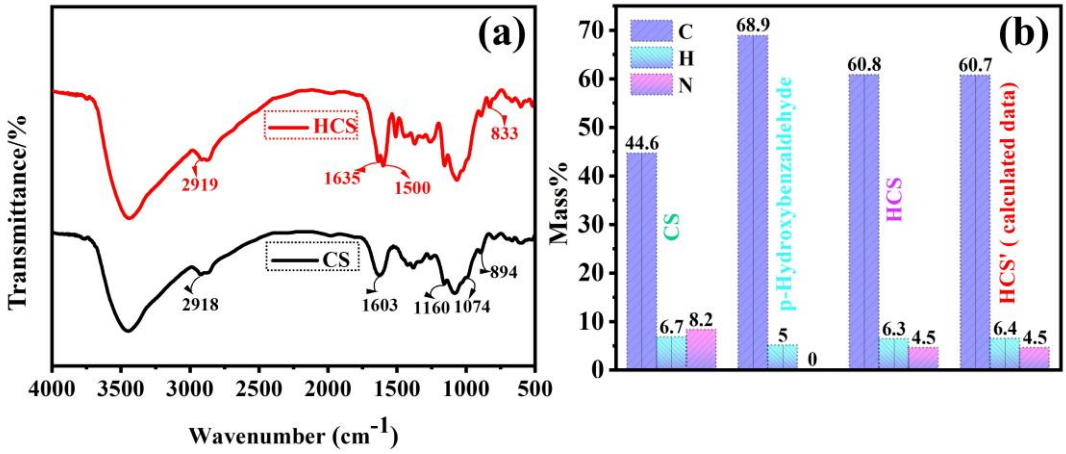

Fig. 2 (**a**) FTIR spectra, (**b**) element analysis and calculated data of CS and HCS samples

Based on our previous work [23], the mass ratios of chitosan (m_1) to p-hydroxybenzaldehyde (m_2) can be determined quantitatively by calculation (details in the Supplementary Material). Where C, H and O were obtained from elemental analysis, which was shown in Fig. 2(b). The reaction is as follows:

$$R_1 - NH_2 + R_2 - CHO \rightarrow R_1 - N = CH - R_2 + H_2O$$

The m_1/m_2 was calculated to be 1.037.

Thermal stability characterization of EP composites

Fluctuations in the glass transition temperature (T_g) affect the serviceability and processability of the material. T_g of the modified composites was determined by DSC testing. As shown in

Fig. 3(a), the T_g of EP was as high as 160.5 °C. Additions of CS and/or DOPO decreased the T_g values of the EPs. Especially in the case of the addition of DOPO (sample S6), the T_g value significantly reduced to 136.8 °C. Meanwhile, the T_g value of the sample with HCS (sample S7) decreased slightly to 156.7 °C, and the T_g value of sample S4 was 144.3 °C. These results could be explained: I) the addition of HCS and DOPO indirectly reduced the amount of EP added; II), the space-site resistance structure of DOPO reduced the cross-link density of the modified EP materials. The polymer HCS is rich in hydroxyl groups, which may participate in the curing of EP, thus the cross-link density was reduced to a lesser extent. At a total addition of 5 wt % and a mass ratio of HCS/DOPO of 1:3, the composite flame retardant formed a dense cross-linked structure with EPs. These results were consistent with the mechanical properties of sample S4.

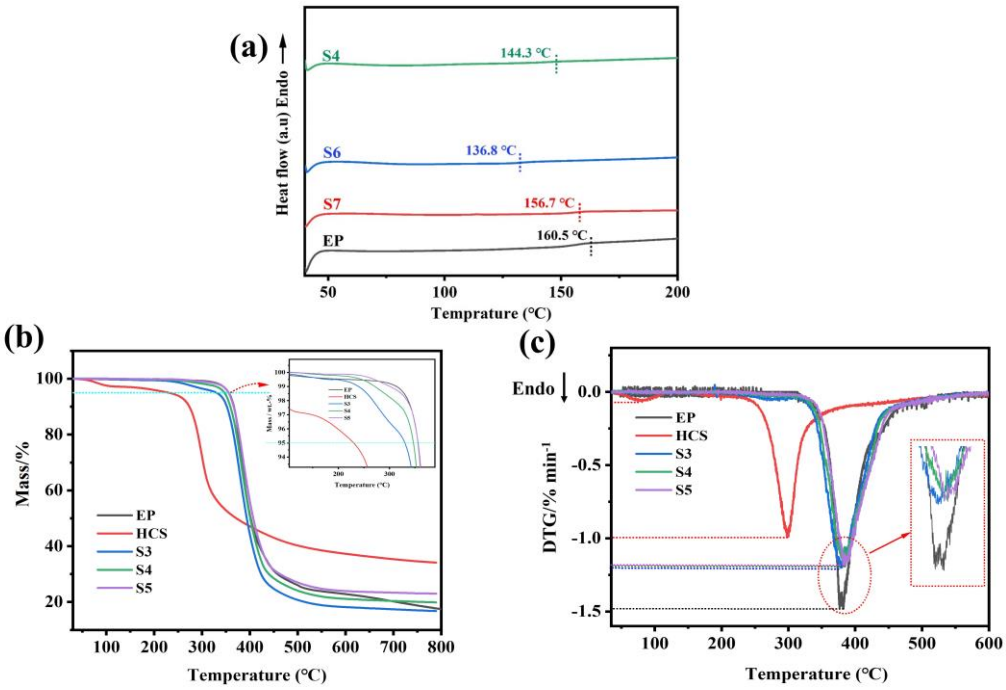

Fig. 3 (**a**) DSC, (**b**) TGA and (**c**) DTG curves of flame-retardant epoxy resin composite under nitrogen atmosphere, and mechanical properties of EP and EP/HCS/DOPO materials

Furthermore, TGA was used to analysis the thermal stability and thermal decomposition behavior of the modified EPs. The TGA curve and the derivative thermogravimetry analysis (DTG) curve of the samples were shown in Fig. 3(b) and Fig. 3(c), respectively, and the results were listed in Table 2. Fig. 3(a) showed that the initial decomposition temperature ($T_{5\%}$) and maximum mass loss temperature ($T_{max\,\%}$) of EP under N_2 atmosphere were 355.8 °C and 380.5 °C, respectively. The $T_{5\%}$ and $T_{max\%}$ of sample S4 were 346.7 °C and 382.9 °C respectively. The $T_{5\%}$ of all modified EPs was higher than the curing temperature (100-150 °C) for the EPs, indicating that DOPO, HCS and HCS/DOPO were all able to comply with the curing conditions. All other samples showed reduction in $T_{5\%}$, but little change in $T_{max\%}$. In addition, the thermal stability of sample S5 was higher than the other two modified EP samples, indicating that the increase in the total addition improved the thermal stability of the material at a 1:3 mass ratio of HCS and DOPO.

The DTG curves of sample EP and S4 were presented in Fig. 3(c). These results demonstrated that sample S4 not only had a higher residual mass than EP at 800 °C, but also had a lower T_{max}. To quantify the carbon-forming capacity more concretely, calculated values of the char residue mass (W_{cal}) were obtained according to equation (1):

$$W_{cal}(T) = \sum_{i=1}^{n} x_i W_i(T) \qquad (1)$$

In this equation, W_i, and x_i represent the residual mass of individual samples from the TGA test and their raw material components, respectively. W_{exp} is the experimental value of residual mass, ΔW is the difference between W_{exp} and W_{cal}. The detailed results were presented in Table 2, the modified EP samples exhibited an enhanced carbon formation capacity. The possible reason was that HCS containing polyhydroxy groups and DOPO containing reactive P-H groups participated in the curing reaction of EP，increasing the crosslink density of the epoxy resin. However, the addition of both also indirectly reduced the content of epoxy groups. As the addition of HCS and DOPO increased, the char residues of sample S4 and sample S5 at 800°C were higher than those of EP, indicating that these modified epoxies had a higher charring capacity than EP.

Table 2 TGA and DTG results of EP samples under nitrogen atmosphere

Sample	$T_{5\%}$ (°C)	T_{max} (°C)	W_{exp} at 800 °C/%	W_{cal} at 800 °C/%	ΔW at 800 °C/%
HCS	224.3	378.6	34.1	/	/
EP	355.8	380.5	17.5	/	/
S3	329.9	383.3	16.8	17.48	-0.68
S4	346.7	382.9	19.9	17.62	2.28

S5	355.4	378.6	23.0	17.94	5.06

Flame retardancy performance

As a first step, EP and modified EPs were tested for UL-94 rating and LOI. EP had an LOI value of 22.6 % and showed no success in the UL-94 test, and was readily combustible. However, with the increase of HCS and/ or DOPO content, the flame retardancy of the thermoset material improved.

As shown in Fig. 4(a), the LOI value for sample S7 was 25.4% when HCS was added at 5%, which was not a significant improvement and failed the UL-94 test. Although the LOI value of S6 sample had been considerably improved to 32.3 %, it only passed the UL-94 V-1 rating. At a total addition of 5% and a 1:3 mass ratio of HCS to DOPO, sample S4 achieved a LOI of 33.0% and successfully passed the UL-94 V-0 rating. The LOI of sample S5 was further increased to 34.5% and passed UL-94 V-0 rating when the content of HCS and DOPO was further increased to 8%. These above results demonstrate that the combination of HCS and DOPO can bestow good flame retardancy on EP.

The cone calorimeter (CC) test is an effective test method for quantitatively evaluating the combustion properties of materials, and series of important parameters can be obtained, such as THR, PHRR, ignition time (TTI), TSP, PSPR, peak time of heat release (t_p), fire growth rate index (FIGRA), av-EHC, average carbon dioxide production rate (av-CO_2Y) and

average carbon monoxide production rate (av-COY), etc. The detailed CC tests results were presented in Table 3, the ignition time of sample S4 was significantly improved compared to that of EP due to the presence of unreacted HCS in the modified EPs. These unreacted HCS thermally decompose to produce some non-combustible substances such as H_2O, NH_3, CO_2 and N_2 at the early stage, diluting the combustible gases on the surface of the material and thus slowing down the combustion of the substrate. As shown in Fig. 4(b), the PHRR of sample S4 was 833.4 KW m^{-2}, a reduction of 21.6 % compared to EP. This was attributed to the dilution of combustible gases by the non-combustible gases generated by sample S4, the absorption of heat by gas diffusion and moisture evaporation, and the promotion of early and rapid coking of the substrate surface to barrier the transfer of heat. To evaluate the fire safety of the material intuitively, FIGRA was investigated, which is equal to PHRR/t_p. The FIGRA value of sample S4 was 6.2, which was lower than that of EP (8.3), indicating that the more adequate escape time in an actual fire situation for sample S4. In addition, the S4 sample had the lowest THR value, with a decrease of approximately 12.3 % compared to EP, as is shown in Fig. 4(c). On the other hand, the value of PSPR and TSP for sample S4 in Fig. 4(d, e) decreased by 21.6 % and 71.4 %, respectively, compared with EP. All these results illustrated that the addition of HCS and DOPO generated a good smoke suppression effect on EP. Meanwhile, the av-EHC value of sample S4 was 31.4 MJ kg^{-1}, which was comparable to that

of EP (32.5 MJ kg^{-1}). The flame retardancy effect of sample S4 in the gas phase during combustion was slight poor, whileas the flame retardancy effect was important in the condensed phase. The char residue mass of sample S4 was increased by 158.6 % compared to that of EP, further verifying the leading role of flame retardancy effect in the condensed phase.

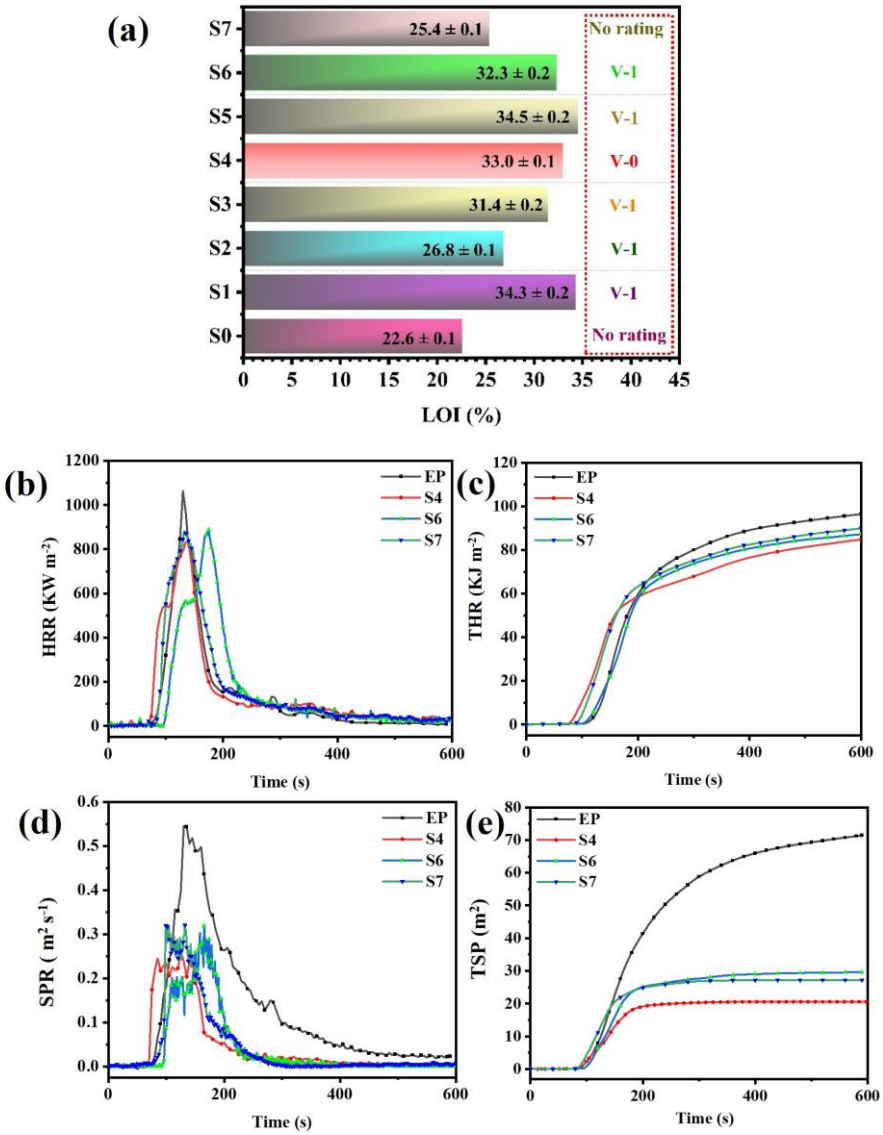

Fig. 4 (**a**) UL-94 and LOI, (**b**) the curves of HRR, (**c**) THR, (d) SPR and (**e**) TSP of EP and modified EPs

Furthermore, there are other patterns to quantify the flame retardancy effect, such as flame inhibition effect, charring effect and barrier and protective effect. Calculated as the following equations (2)-(4) [30]:

$$\text{Flame inhibition} = 1 - EHC_{modified\ EP}/EHC_{EP} \quad (2)$$

$$\text{Charring effect} = 1 - TML_{modified\ EP}/TML_{EP} \quad (3)$$

$$\text{Barrier and protective effect} = 1 - \frac{PHRR_{modified\ EP}/PHRR_{EP}}{THR_{modified\ EP}/THR_{EP}} \quad (4)$$

These results were also summarized in Table 3. The flame inhibition effect of sample S6 was the best, but the barrier and protective effect was the worst, which confirmed that DOPO was mainly manifested in the gas-phase flame retardation mechanism. However, the sample S4 modified by HCS and DOPO flame retardant was manifested in condensed phase flame retardancy mechanism.

Table 3 The CC tests results of EP and its flame-retardant EP samples

Sample	EP	S4	S6	S7
TTI (s)	59 ± 3	76 ± 3	96 ± 2	81 ± 3
t_P (s)	130 ± 2	135 ± 2	174 ±2	132 ± 3
PHRR (KW m^{-2})	1063.1 ± 20	833.4 ± 14	889.4 ± 14	881.3 ± 15
FIGRA	8.3 ± 0.1	6.2 ± 0.2	5.1 ± 0.1	6.6 ± 0.1

THR (MJ m^{-2})	96.5 ± 3	84.6 ± 3	87.3 ± 3	89.8 ± 4
PSPR (m^2 s^{-1})	0.55± 0.02	0.25 ± 0.02	0.32 ± 0.02	0.33 ± 0.02
TSP (m^2)	71.4 ± 0.3	20.4 ± 0.3	29.6 ± 0.3	27.1 ± 0.3
av-EHC (MJ kg^{-1})	32.5 ± 0.4	31.4 ± 0.4	26.3 ± 0.2	31.8 ± 0.3
av-COY (kg kg^{-1})	0.33 ± 0.02	0.24 ± 0.02	0.22 ± 0.02	0.35 ± 0.02
av-CO_2Y (kg kg^{-1})	1.4 ± 0.1	2.7 ± 0.2	3.4 ± 0.2	3.5 ± 0.2
TML (%)	89.6	73.1	80.3	83.8
Char residue (%)	10.4	26.9	19.7	16.2
Flame inhibition (%)	/	3.4	19.1	7.3
Charring effect (%)	/	18.4	10.4	6.5
Barrier and protective effect (%)	/	10.6	7.5	11.0

Flame retardancy mechanism analysis

Firstly, the gas phase flame retardancy mechanism was investigated by employing Py-GCMS and TG-IR tests on the modified EPs. In general, DOPO is thermally decomposed during combustion, releasing radicals containing P and thus acting as a flame retardant in the gas phase. Py-GC/MS tests were carried out on EP and sample S4 to investigate the gaseous flame retardancy mechanism at 500 °C. As shown in Fig. S1 and Table S1, the main pyrolysis

products of neat EP samples were DDM and EP derivatives. Among them, the ·OH and ·H radicals generated during the thermal cracking process were the major contributors to the flammability of the thermosetting EPs. Fig. 5 showed the pyrolysis spectrum of sample S4 and some of the identified specific pyrolysis products. Some characteristic products of S4 were as follows: carbon dioxide (a), $\cdot PO_2$ free radical (b), phenol (c), (4-hydroxyphenyl) phosphonic acid (d), m-cresol (e), 3-isopropylphenol (f), 4-(prop-1-en-2-yl)phenol (g), 1,1'-biphenyl (h), 2-methyl-1,1'-biphenyl (i), 3-benzylaniline (j), 4-(2-phenylpropan-2-yl)phenol (k), 4-(2-(4-methoxyphenyl)propan-2-yl)phenol (l), 4,4'-(propane-2,2-diyl)diphenol (m), bis(4-(prop-1-en-2-yl)phenyl)methane (n), 3,3',4,4',5,5'-hexamethyl-1,1'-biphenyl (o), bis(4-isopropylphenyl)methane (p), 9H-fluorene (q), N-phenylphenanthridin-6-amine (r). Considering the structure of HCS/DOPO flame retardants, the pyrolysis products (h, i, q, r) were considered to be attributable to the decomposition of DOPO, accompanied by the production of ·PO and $\cdot PO_2$ (b) radicals. By capturing the reactive radicals during combustion, such phosphorus-containing radicals serve to terminate the free radical chain reaction. The peaks (c, d, g) predominantly correlate to the cleavage of chitosan fragments in HCS. Peaks with retention times greater than 20.0 min were also present in the cracking spectrum of sample S4 compared to EP, suggesting that the substances identified with these peaks have a similar cracking composition to EP. Flame

retardant compounds can produce non-combustible gases such as CO_2, H_2O and NH_3 which dilute combustible gases in the vicinity of the substrate and transfer significant amounts of heat away. According to the foregoing studies, the flame retardancy mechanism of sample S4 was presumably summarized as follows: i) during the thermal decomposition stages, the stepwise decomposition of DOPO and HCS contributed to the release of phosphorus-containing radicals and non-combustible gases, which acted as quenchers and diluents in the gas phase, respectively; ii) some of the thermal decomposition products of HCS were mostly retained after reacting with the phosphorus-containing compounds produced by the decomposition of DOPO in the condensed phase, which can catalyze the accelerated formation of more dense char layers, and these char layers can provide a good thermo-oxygen barrier effect.

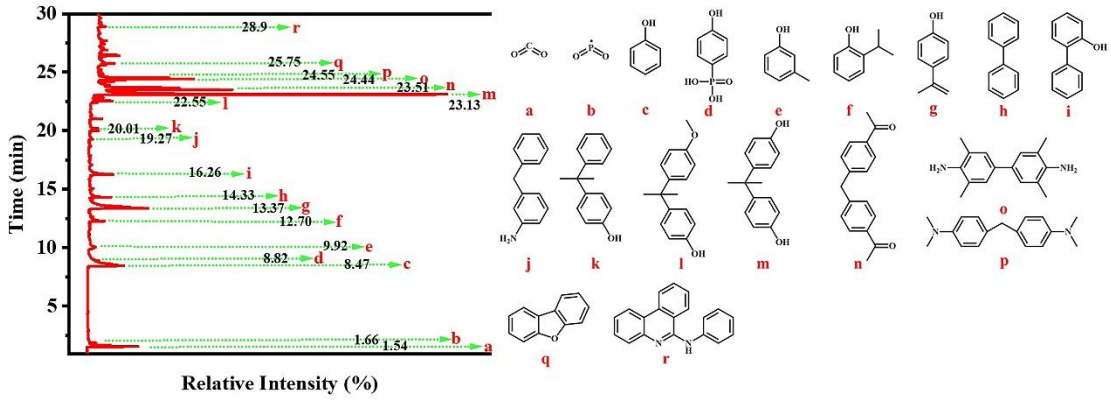

Fig. 5 Pyrolysis mass spectrum of sample S4 and partially identified cracking compounds

The TG-FTIR spectra were used to further investigate the flame retardancy mechanism of sample S4. Fig. 6 showed the TG-FTIR spectra of the pyrolysis gas products of the EP and

S4 samples at 300 °C, 350 °C, 400 °C, 450 °C, 500 °C, 550 °C and 600 °C, respectively. As shown in Fig. 6(a, c), the characteristic absorption peaks of some thermally crazed molecules can be identified easily in EP sample, such as Ph-O-C (1260 cm^{-1}), C=O (1740 cm^{-1}), carbon dioxide (2360 cm^{-1}) and hydrocarbons (2970 cm^{-1}, 1180 cm^{-1}). Water can be directly identified in the spectral peaks of 4000~3500 cm^{-1} and 1300~1600 cm^{-1} [31-33]. Fig. 6(b, d) showed the FTIR spectra of the pyrolysis gas products of sample S4, the peaks at 1260 cm^{-1} and 1130 cm^{-1} were attributed to the Ph-O-C and Ph-P bond, respectively, which may overlap with the characteristic absorbance of the ether bond [34, 35]. Phosphorus-containing fragments can clearly be seen in the pyrolysis gas from sample S4, indicating that the HCS/DOPO flame retardant system played a flame retardancy role in the gas phase, which was consistent with the findings of the Py-GCMS.

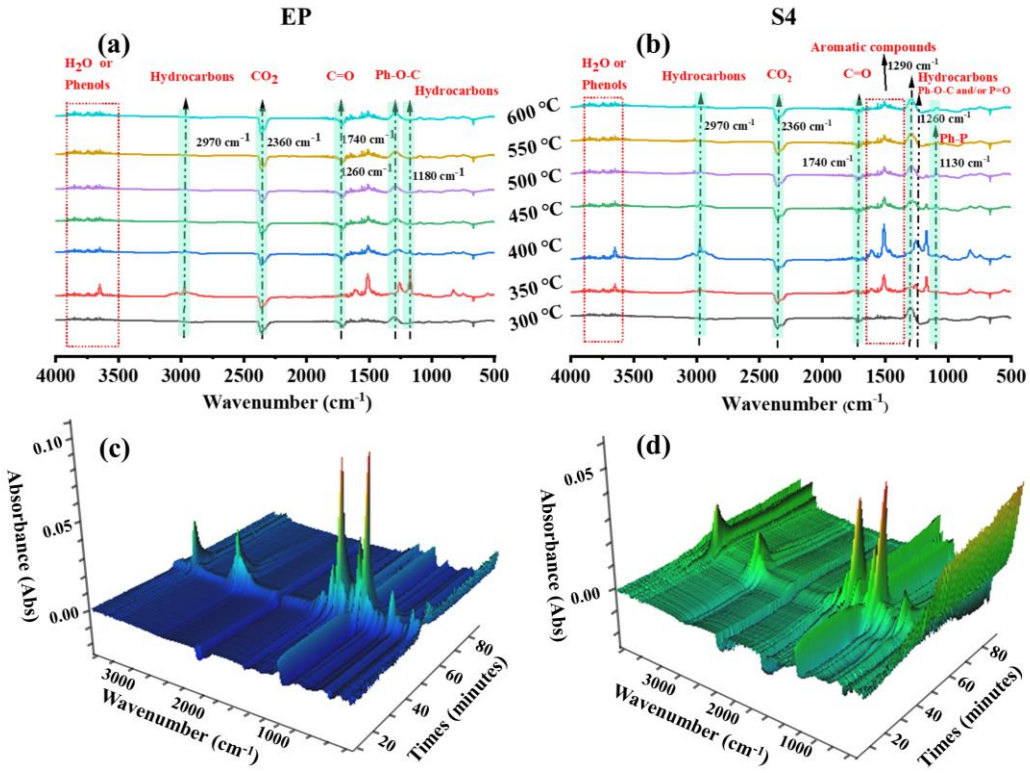

Fig. 6 The FTIR spectra of (**a**) EP and (**b**) S4 samples at different temperatures, and 3D TG-FTIR spectra of pyrolysis products of (**c**) EP and (**d**) S4 samples

Secondly, a series of characterizations of the char residual after CC testing was used to reveal the mechanism of the condensed phase flame retardancy action. In Fig. 7(a, a-1, b, b-1), EP was almost completely burned out, resulting in a sparse and discontinuous char residue with a height of about 1.8 cm, while the expansive char residue formed by sample S4 was compact and intact with a height of about 3.1 cm. There is no doubt that this massive expandable char layer acted as a good barrier to the transfer of heat and oxygen, covering the surface of the matrix and thus slowing the combustion of the matrix. The flame retardancy mechanism of condensed phase was further verified. Fig. 7(a-2, a-3, a-4) and (b-2, b-3, b-4)

showed the SEM digital images of the char residue after CC tests for EP and S4 samples respectively. It is plain to see from the images that the char layer of EP was rough and showed a number of visible gaps, whereas the char layer of sample S4 was much denser and smoother, with a glassy surface and a very well-sealed. It acted as a barrier and better prevented the transfer of oxygen and heat. In order to elucidate the reasons for the formation of dense carbon layers, Raman spectroscopy was first used to analyze the degree of disorder in the structure of the carbonaceous material, in the other words, the degree of graphitization of the carbon layers. In Fig. 8, two peaks appeared in both spectra near 1360 cm^{-1} and 1601 cm^{-1}, belonging to the D-band formed by disordered graphite or amorphous carbon vibrations and the G-band belonging to sp^{2-} hybridized aromatic layer-vibrations [36]. The degree of graphitization is usually evaluated by the ratio of the integral strength of the D and G bonds, which is inversely proportional to the R value ($R=I_D/I_G$), the R value of sample S4 was 3.63, which was lower than that of EP (4.03). Therefore, sample S4 was concluded to have a denser carbon layer and a higher degree of graphitization, which was consistent with the SEM results.

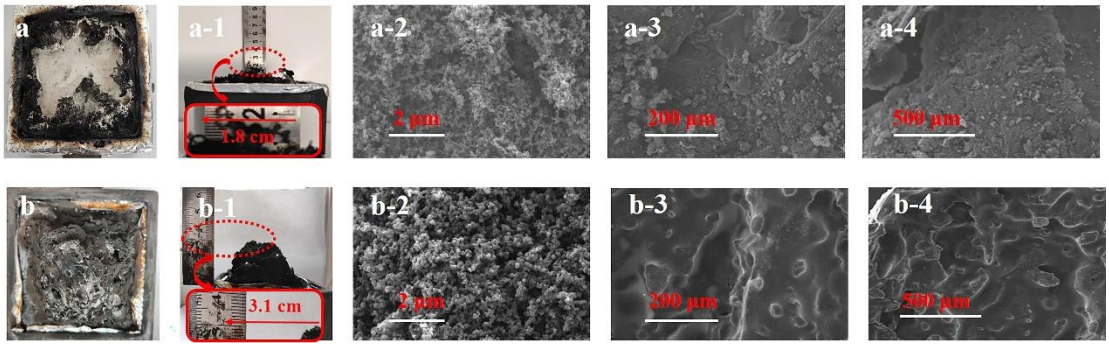

Fig. 7 Char residue (**a**, **a-1**, **b**, **b-1**) and SEM digital images (**a-2**, **a-3**, **a-4**, **b-2**, **b-3**, **b-4**) of EP and S4 samples after CC tests

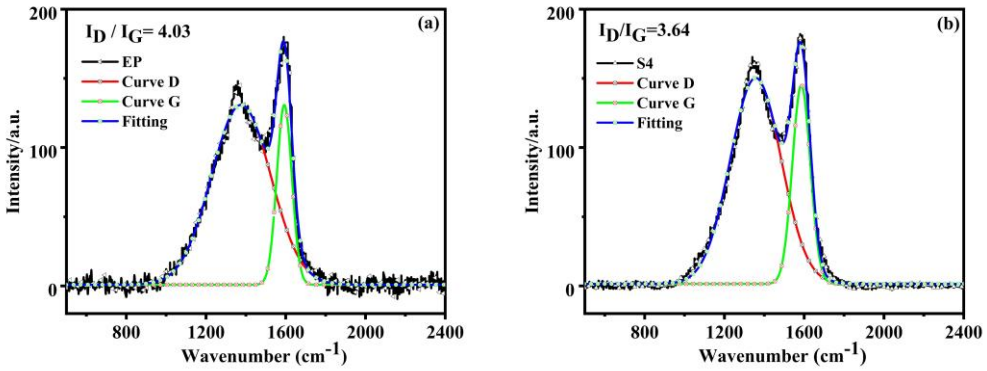

Fig. 8 Raman spectra of char residues for EP and S4 samples

The scientific investigation of the chemical composition of the char residue was essential. The char residue of sample S4 was analyzed using EDX and the results were shown in Fig. 9(a). The presence of significant phosphorus containing material in the char residue has a high phosphorus content of 12.07 %. Fig. 9(b) showed the element content of char residues for EP and S4 samples. The absorption peaks at 2924 cm^{-1}, 1621 cm^{-1} and 1074 cm^{-1} were stretching vibrations of -CH_2-, C=C and C-N bonds, respectively [37, 38]. The FTIR of sample S4 was significantly different from that of EP, with phenol being identified at 1513

cm^{-1}. P=O and P-O-C stretching vibrations were visible at 1234 cm^{-1} and 1166 cm^{-1}, respectively, further verifying the presence of phosphorus oxides and organophosphorus compounds in the char residue [39, 40]. It indicated that phosphorus-containing compounds, which is capable of accelerating the cross-linking of EP degradation products, were produced during the combustion of sample S4, and dense and stable char residues were obtained.

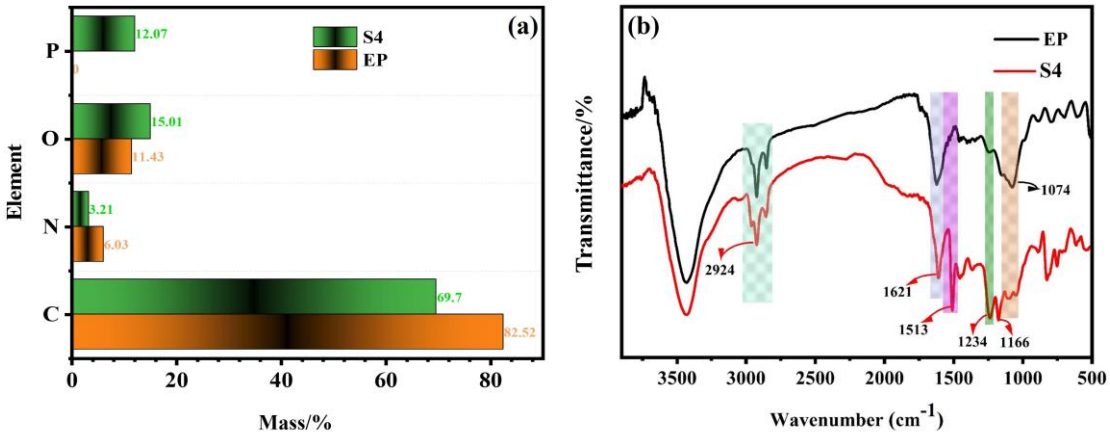

Fig. 9 FTIR spectra and element content of char residues for EP and S4 samples

The C_{1s} spectra of EP and S4 samples were shown in Fig. 10(b, c), and the percentages of each bond were shown in Table S2. Three carbon binding states were observed in the C_{1s} spectra of two samples. The peaks near 288.0 eV belonged to C=O bond, the peaks near 285.7 eV belonged to C-O bond in hydroxyl and/or carbonyl, and the peaks near 284.7 eV belonged to C-C bond in aliphatic and aromatic components (C_a) [41-43]. According to the literature, C-O and C=O can be referred to as carbon oxides (C_{ox}). The C_{ox}/C_a ratio was used to evaluate the thermal oxidation properties of the residual carbon [44]. As shown in Table S2, the C_{ox}/C_a ratios of the samples were EP (0.85) > S4 (0.75). The C_{ox}/C_a ratios of the three modified EPs

were lower than that of EP, indicating that the thermal oxidation of the char residual of the modified epoxy resin was enhanced, which could be used as a protective barrier for the thermal oxygen consumption of the matrix.

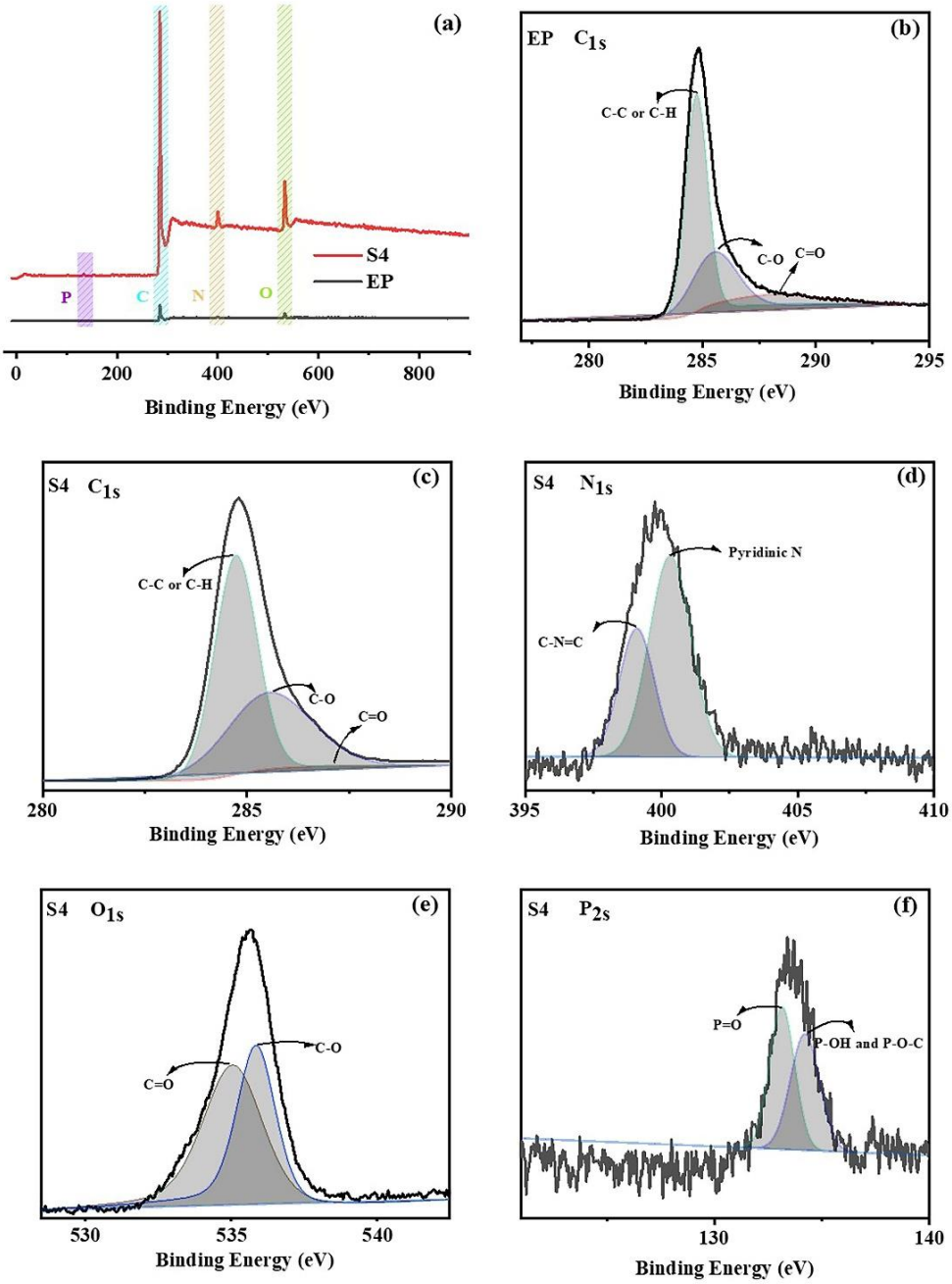

Fig. 10 The high-resolution XPS spectra (**a**) of char residue for EP at (**b**) C_{1s} region and sample S4 at (**c**) C_{1s}, (**d**) N_{1s}, (**e**) O_{1s} and (**f**) P_{2p} regions

A possible flame retardancy mechanism of HCS/DOPO (see Fig. 11) was postulated based on the above analysis as follows: (i) DOPO decomposed during combustion, releasing phosphorus-based fragments, such as ·PO and $\cdot PO_2$ radicals, which inhibited the combustion reaction at the surface of the thermosetting resin. Simultaneously, HCS thermally decomposes into non-combustible gases such as H_2O, N_2, NH_3 and CO_2 as diluents for combustible gases; (ii) The degradation of DOPO produced phosphorus-containing compounds with catalytic effect, which promoted the char-forming properties of the EP matrix [45, 46]. Not only that, the addition of HCS could also promote the formation of highly dense graphitized char layers of EP, with a much higher generation of char residues and better heat and mass transfer barriers. In summary, it was hypothesized that the HCS/DOPO modified EP could exhibit flame retardancy in both the gas phase and condensed phase, with the condensed phase flame retardancy mechanism being at an advantage.

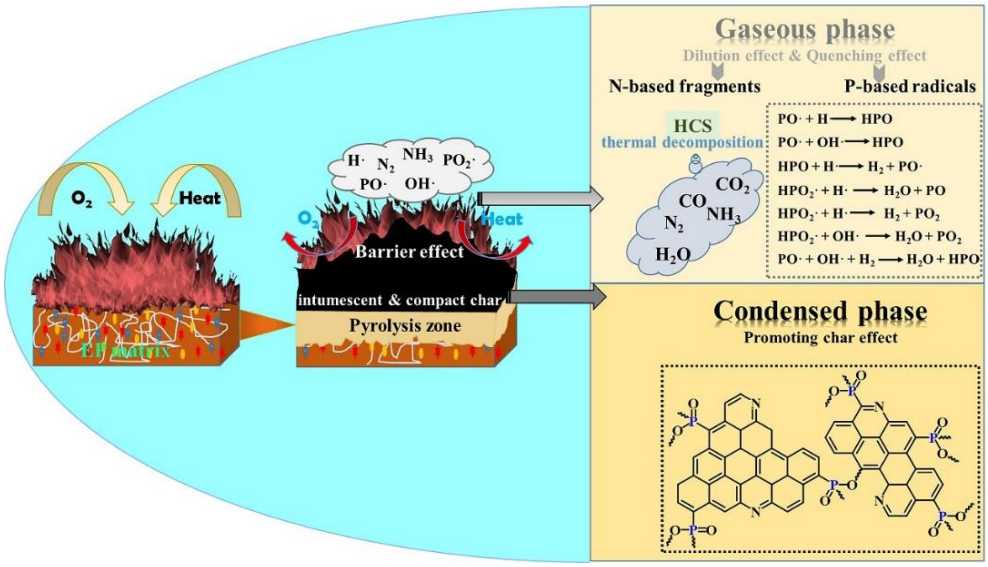

Fig. 11 Possible flame retardancy mode-of-action of EP/HCS/DOPO

Mechanical performance

In general, the addition of most additive flame retardants, while enhancing the flame retardancy of EP, can reduce the mechanical properties of the modified materials, thus indirectly limiting the application of EP. Therefore, some detection of mechanical properties (tensile and three-point bending tests) is considered necessary. The detail tests data was shown in Fig. 12. Compared to the EP-only samples, neither of the samples with the addition of HCS and DOPO alone showed any significant loss of mechanical properties, changing little. In contrast, as shown in the Fig. 12, sample S4 showed a significant increase in both tensile and flexural strengths, which was attributable to the good compatibility of HCS/DOPO with EP at the addition amount. From the perspective of chemical reactions, many of the reactive groups in the compounded flame retardant (-PH bond in DOPO; -CH_2OH, phenolic hydroxyl groups and unreacted NH_2 in HCS) can react with the epoxy groups. As can be seen from the results, although the addition of HCS and DOPO alone reduced the degree of crosslinking of the modified epoxy resin, the synergistic effect of HCS and DOPO could well compensate for the deficiencies in mechanical properties. In addition, the stacking effect of π-π interactions between aromatic rings (including DOPO) in modified EP had positive effects on the improvement of mechanical properties [47, 48]. Based on the above analysis,

the possible interactions between HCS/DOPO and EP were postulated, as shown in Fig. 1(c).

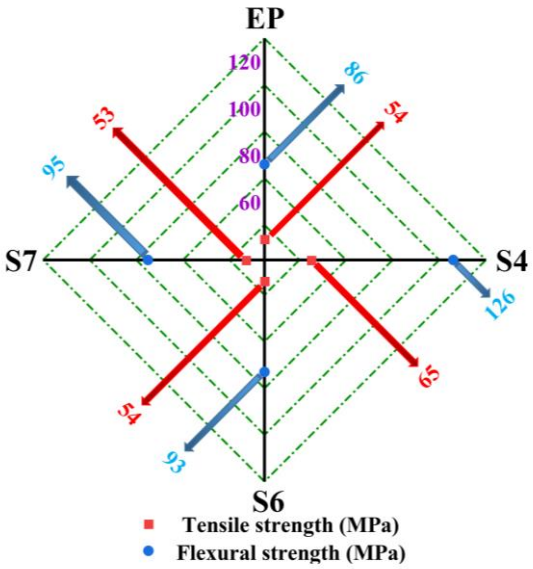

Fig. 12 The mechanical properties of the modified materials

CONCLUSIONS

In this work, a flame-retardant precursor HCS, rich in active hydroxyl groups, was successfully synthesized from the biological material chitosan and p-hydroxybenzaldehyde, and the synthesized HCS was compounded with DOPO to obtain a good IFR for EP. At a total flame retardant addition of 5 mass% and a mass ratio of 1:3 between HCS and DOPO, the modified EP passed the UL-94 V-0 rating with an LOI value of up to 34.5 %. The CC data revealed that the introduction of precursors and DOPO into EP enabled high efficiency flame retardancy, good smoke suppression, a delayed ignition time, and a significant increase (an increase of 158.6 %) in char residue generation. The THR, PSPR and TSP were all reduced compared with those with HCS or DOPO alone, indicating that HCS and DOPO had good

synergistic flame retardancy. In addition, the flame retardancy mechanism of the modified epoxy resin was investigated in the gas phase and condensed phase, respectively. These results showed that HCS/DOPO had flame retardancy in both the condensed and gas phases, with the condensed phase dominating the flame retardancy mechanism. In conclusion, the synergistic effect of HCS and DOPO was excellent and significantly enhanced the flame retardancy of EP, especially the smoke suppression properties. Meanwhile, HCS/DOPO was well compatibility with EP and the mechanical properties were improved.

Acknowledgments This work was supported by the Open Fund of Hubei Key Laboratory for New Textile Materials and Applications (Wuhan Textile University, 247052).

Author contributions Jing Yan contributed to methodology, data curation and writing-review. Haiqing Jiang and Na Gao contributed to experiment, data curation, investigation and writing-original draft preparation. Xiangnan Zhang contributed to visualization and writing-review and editing. Xingyu Liu contributed to conceptualization, methodology, writing-review and editing. Siqi Huo contributed to methodology and supervision. Jing Lu and Junjie Wang contributed to conceptualization and resources.

Declarations

Conflict of interest The authors declare that they have no known competing financial interests or personal relationships that could have appeared to influence the work reported in this paper.

Data and code availability

The raw and processed data generated during this study will be made available upon reasonable request.

References

1. Wang Y, Ma L, Yuan J, Yin XZ, Wang H, Cheng CZ, Wang LX, Zhu ZM, Weng YX. A green flame retardant by elaborate designing towards multifunctional fire-safety epoxy resin composites. React Funct Polym. 2022;180:105390.
2. Wang JJ, Chen JH, Wang WW, Lu J, Li YY, Bai T, Chen JH, Zhu ZM, Wang D. Preparation of boron-containing chitosan derivative and its application as intumescent flame retardant for epoxy resin. Cellulose. 2023;30:4663-4681.
3. Ye GF, Huo SQ, Wang C, Song PA, Fang ZP, Wang H, Liu Z. Durable flame-retardant, strong and tough epoxy resins with well-preserved thermal and optical properties via introducing a bio-based, phosphorus-phosphorus, hyperbranched oligomer. Polym Degrad Stabil. 2023;207:110235.

4. Toldy A, Szlancsik A, Szolnoki B. Reactive flame retardancy of cyanate ester/epoxy resin blends and their carbon fibre reinforced composites. Polym Degrad Stabil. 2016;128:29-38.

5. Han GJ, Zhao XY, Feng YZ, Ma JM, Zhou KQ, Shi YQ, Liu CT, Xie XL. Highly Flame-retardant Epoxy-based Thermal Conductive Composites with Functionalized Boron Nitride Nanosheets Exfoliated by One-Step Ball Milling. Chem Eng J. 2020;407(17):127099.

6. Lu SY, Hamerton I. Recent developments in the chemistry of halogen-free flame retardant polymers. Prog Polym Sci. 2002;27:1661-1712.

7. Gao LP, Wang DY, Wang YZ, Wang JS, Yang B. A flame-retardant epoxy resin based on a reactive phosphorus-containing monomer of DODPP and its thermal and flame-retardant properties. Polym Degrad Stabil. 2008;93:1308-1315.

8. Wang JJ, Tang H, Yu XJ, Xu J, Pan ZQ, Zhou H. Reactive organophosphorus flame retardant for transparency, low-flammability, and mechanical reinforcement epoxy resin. J Appl Polym Sci. 2021;138:50536.

9. Sun ZZ, Hou YB, Hu Y, Hu WZ. Effect of additive phosphorus-nitrogen containing flame retardant on char formation and flame retardancy of epoxy resin. Mater Chem Phys. 2018;214:154-164.

10. Gooneie A, Simonetti P, Salmeia KA, Gaan S, Hufenus R, Heuberger MP. Enhanced PET processing with organophosphorus additive: Flame retardant products with added-value for recycling. Polym Degrad Stabil. 2019;160:218-228.
11. Wang P, Xia L, Jian RK, Ai YF, Zheng XL, Chen GL, Wang JS. Flame-retarding epoxy resin with an efficient P/N/S-containing flame retardant: Preparation, thermal stability, and flame retardance. Polym Degrad Stabil. 2018;149:69-77.
12. Huo SQ, Sai T, Ran SY, Guo ZH, Fang ZP, Song PA, Wang H. A hyperbranched P/N/B-containing oligomer as multifunctional flame retardant for epoxy resins. Compos Part B-Eng. 2022;234:109701.
13. Wang C, Huo SQ, Ye GF, Song PA, Wang H, Liu ZT. A P/Si-containing polyethylenimine curing agent towards transparent, durable fire-safe, mechanically-robust and tough epoxy resins. Chem Eng J. 2023;451:138768.
14. Shi Q, Huo SQ, Wang C, Ye GF, Yu LF, Fang ZP, Wang H, Liu ZT. A phosphorus/silicon-based, hyperbranched polymer for high-performance, fire-safe, transparent epoxy resins. Polym Degrad Stabil. 2022;203:110065.
15. Cao JF, Duan HJ, Zou JH, Zhang JJ, Wan C, Zhang CH, Ma HR. Bio-based phosphorus-containing benzoxazine towards high fire safety, heat resistance and mechanical properties of anhydride-cured epoxy resin. Polym Degrad Stabil.

2022;198:109878.

16. Hu P, Zheng XY, Zhu JW, Wu BL. Effects of chicken feather keratin on smoke suppression characteristics and flame retardancy of epoxy resin. Polym Adv Technol. 2020;31:2480-2491.

17. Yang S, Wang J, Huo SQ, Wang M, Wang JP, Zhang B. Synergistic flame-retardant effect of expandable graphite and phosphorus-containing compounds for epoxy resin: Strong bonding of different carbon residues. Polym Degrad Stabil. 2016;128:89-98.

18. Wang JY, Qian LJ, Huang ZG, Fang YY, Qiu Y. Synergistic flame-retardant behavior and mechanisms of aluminum poly-hexamethylenephosphinate and phosphaphenanthrene in epoxy resin. Polym Degrad Stabil. 2016;130:173-181.

19. Zhang L, Wang YC, Liu Q, Cai XF. Synergistic effects between silicon-containing flame retardant and DOPO on flame retardancy of epoxy resins. J Therm Anal Calorim. 2016;123:1343-1350.

20. Zeng BR, Yang L, Chen JM, Liu XY, Wu HY, Zheng W, Chen GR, Xu YT, Dai LZ. Improving the flame retardancy and thermal property of organotitanate-modified epoxy resin for electronic application via a simple method. High Perform Polym. 2019;31(1):12-23.

21. Luo H, Zhou F, Yang YY, Cao XL, Cai XF. Synergistic flame-retardant behavior and

mechanism of tris (3-nitrophenyl) phosphine and DOPO in epoxy resins. J Therm Anal Calorim. 2018;132:483-491.

22. Chen R, Hu KX, Tang H, Wang JJ, Zhu FS, Zhou H. A novel flame retardant derived from DOPO and piperazine and its application in epoxy resin: Flame retardance, thermal stability and pyrolysis behavior. Polym Degrad Stabil. 2019;166:334-343.

23. Wang JJ, Yu XJ, Dai SS, Wang XY, Pan ZQ, Zhou H. Synergistic effect of chitosan derivative and DOPO for simultaneous improvement of flame retardancy and mechanical property of epoxy resin. Cellulose. 2022;29:907-925.

24. Wang JT, Lian ZR, Wang HD, Jin XX, Liu YJ. Synthesis and Antimicrobial Activity of Schiff Base of Chitosan and Acylated Chitosan. J Appl Polym Sci. 2012;123:3242-3247.

25. Baran T, Açıksöz E, Mentes A. Carboxymethyl chitosan Schiff base supported heterogeneous palladium (II) catalysts for Suzuki cross-coupling reaction. J Mol Catal A-Chem. 2015;407:47-52.

26. Ciursă P, Pauliuc D, Dranca F, Ropciuc S, Oroian M. Detection of honey adulterated with agave, corn, inverted sugar, maple and rice syrups using FTIR analysis. Food Control 2021;130:108266.

27. Corazzari I, Nistico R, Turci F, Faga MG, Franzoso F, Tabasso S, Magnacca G. Advanced physico-chemical characterization of chitosan by means of TGA coupled

on-line with FTIR and GCMS: Thermal degradation and water adsorption capacity. Polym Degrad Stabil. 2015;112:1-9.

28. Rhofir C, Le-Thanh H, Vocelle D, Sandorfy C. FTIR study of the protonation of a schiff base in chloroform-methanol mixtures. J Mol Struct. 1989;198:451-460.

29. Lal K, Poonia N, Rani P, Kumar A, Kumar A. Design, synthesis, antimicrobial evaluation and docking studies of urea-triazole-amide hybrids. J Mol Struct. 2020;1215:128234.

30. Tang S, Wachtendorf V, Klack P, Qian LJ, Dong YP, Schartel B. Enhanced flame-retardant effect of a montmorillonite/phosphaphenanthrene compound in an epoxy thermoset. RSC Adv. 2017;7:720-728.

31. Xu F, Zhong L, Xu Y, Zhang C, Zhang FX, Zhang GX. Highly efficient flame-retardant and soft cotton fabric prepared by a novel reactive flame retardant. Cellulose. 2019;26:4225-4240.

32. Liu J, Dong CH, Zhang Z, Kong DZ, Sun H, Lu Z. Multifunctional flame-retarded and hydrophobic cotton fabrics modified with a cyclic phosphorus/polysiloxane copolymer. Cellulose. 2020;27:3531-3549.

33. Chi ZY, Guo ZW, Xu ZC, Zhang MJ, Li M, Shang L, Ao YH. A DOPO-based phosphorus-nitrogen flame retardant bio-based epoxy resin from diphenolic acid: Synthesis, flame-retardant behavior and mechanism. Polym Degrad Stabil.

2020;176:109151.

34. Xu F, Zhong L, Xu Y, Zhang C, Wang P, Zhang FX, Guang X. Synthesis of three novel amino acids-based flame retardants with multiple reactive groups for cotton fabrics. Cellulose. 2019;26:7537-7552.

35. Zhang JJ, Duan HJ, Cao JF, Zou JH, Ma HR. A high-efficiency DOPO-based reactive flame retardant with bi-hydroxyl for low-flammability epoxy resin. J Appl Polym Sci. 2020;138:50165.

36. Ai LH, Chen SS, Zeng JM, Liu P, Liu WS, Pan YH, Liu D. Synthesis and flame retardant properties of cyclophosphazene derivatives containing boron. Polym Degrad Stabil. 2018;155:250-261.

37. Liu C, Huang JM, Zhu JH, Yuan CH, Zeng BR, Chen GR, Xu YT, Dai LZ. Synthesis of a novel azaphosphorine flame retardant and its application in epoxy resins. J Appl Polym Sci. 2018;135:45721.

38. Huang YW, Yang Y, Ma JJ, Yang JX. Preparation of ferric phosphonate/phosphinate and their special action on flame retardancy of epoxy resin. J Appl Polym Sci. 2018;135:46206.

39. Shao ZB, Zhang MX, Li Y, Han Y, Ren L, Deng C. A Novel Multi-Functional Polymeric Curing Agent: Synthesis, Characterization, and Its Epoxy Resin with Simultaneous

Excellent Flame Retardance and Transparency. Chem Eng J. 2018;345:471-482.

40. Perret B, Schartel B, Stöß K, Ciesielski M, Diederichs J, Döring M, Krämer J, Altstädt V. A New Halogen-Free Flame Retardant Based on 9,10-Dihydro-9-oxa-10-phosphaphenanthrene-10-oxide for Epoxy Resins and their Carbon Fiber Composites for the Automotive and Aviation Industries. Macromol Mater Eng. 2011;296:14-30.

41. Xu MJ, Li X, Li B. Synthesis of a novel cross-linked organophosphorus-nitrogen containing polymer and its application in flame retardant epoxy resins. Fire Mater. 2016;40:848-860.

42. Tang QB, Wang BB, Shi YQ, Song L, Hu Y. Microencapsulated Ammonium Polyphosphate with Glycidyl Methacrylate Shell: Application to Flame Retardant Epoxy Resin. Ind Eng Chem Res. 2013;52:5640-5647.

43. Wang JQ, Du JX, Zhu J, Wilkie CA. An XPS study of the thermal degradation and flame retardant mechanism of polystyrene-clay nanocomposites. Polym Degrad Stabil. 2002;77:249-252.

44. Guo WW, Nie SB, Kalali EN, Wang X, Wang W, Cai W, Song L, Hu Y. Construction of SiO_2@UiO-66 core-shell microarchitectures through covalent linkage as flame retardant and smoke suppressant for epoxy resins. Compos Part B-Eng. 2019;176:107261.

45. Li J, Li B, Zhang XC, Su RZ. The study of flame retardants on thermal degradation and charring process of manchurian ash lignin in the condensed phase. Polym Degrad Stabil. 2001;72:493-498.

46. Xie WQ, Huang SW, Tang DL, Liu SM, Zhao JQ. Synthesis of a furfural-based DOPO-containing co-curing agent for fire-safe epoxy resin. RSC Adv. 2020;10:1956-1965.

47. Zhou CY, Wang XY, Wang JJ, Pan ZQ, Zhou H. Epoxy resin modified with chitosan derivatives and DOPO: Improved flame retardancy, mechanical properties and transparency. Polym Degrad Stabil. 2022;199:109931.

48. Luo H, Zhou F, Yang YY, Cao XL, Cai XF. Gas-condensed phase flame-retardant mechanisms of tris(3-nitrophenyl) phosphine/triphenyl phosphate/ABS. J Therm Anal Calorim. 2018;132:263-273.